Journal of Applied Polymer Science

A Complex Based on Imidazole Ionic Liquid and Copolymer of Acrylamide and Phenoxyacetamide Modification for Clay Stabilizer

Pingli Liu,[1] Lihua Zhou,[2] Cheng Yang,[2] Hong Xia,[2] Yang He,[2] Meilin Feng[2]

[1]State Key Laboratory of Oil and Gas Reservoir Geology and Exploitation, Southwest Petroleum University, Chengdu 610500, People's Republic of China

[2]School of Chemistry and Chemical Engineering, Southwest Petroleum University, Chengdu 610500, People's Republic of China

Correspondence to: P.-L. Liu (E-mail: lhzhouswpu@163.com)

ABSTRACT: A complex system (AM/AA/APO-EMIN) was obtained by poly (acrylamide-*co*-acrylic acid-*co*-*N*-allyl-2-phenoxyacetamide) (AM/AA/APO) combining 1-ethyl-3-methyl imidazolium tetrafluoroborate ([EMIM] [BF_4]) for clay stabilizer by using acrylamide (AM), acrylic acid (AA) and *N*-allyl-2-phenoxyacetamide (APO), *N*-methylimidazole, bromoethane, and sodium fluoroborate as raw materials. The complex solution exhibited excellent anti-swelling rate (up to 94.5% at 10,000 mg/L), satisfying aging resistance (viscosity retention rate 84.2% after 15 days), and marked shear thinning behavior (viscosity retention rate 7.5% under 600 s^{-1}). From scanning electron microscope (SEM) images, a clear network structure appeared in AM/AA/APO-EMIM solution. Compared with an existing poly (acrylamide-*co*-diallyl dimethyl ammonium chloride) clay stabilizer (HY-201S), AM/AA/APO-EMIN was less content and more effective to reduce the *d*-spacing of sodium montmorillonite (Na-MMT) from 19.1 Å to 15.7 Å. © 2014 Wiley Periodicals, Inc. J. Appl. Polym. Sci. **2015**, *132*, 41536.

KEYWORDS: copolymers; ionic liquids; oil and gas; polyamides

Received 28 February 2014; accepted 19 September 2014
DOI: 10.1002/app.41536

INTRODUCTION

It has been known that most of the formations faced in petroleum exploitation are shale formations.[1,2] Clay minerals, as a major mineral of shale formations, may occur hydration, swelling and further migration when contacted with the external liquid, which is the main factor causing formation permeability damages and downhole accidents .[3–7] At present, using clay stabilizers has become one of the most common methods to prevent or weaken the hydration.[4,8–10]

According to the chemical components, clay stabilizers can be divided into four categories: inorganic salts and alkalis, inorganic polymers, cationic surfactants, and organic cationic polymers.[4,8,11–13] However, the main problem of small molecule clay stabilizers is poor stability and capacity to inhibit clay particles migration, in spite of remarkable effects of anti-swelling.[8,9] On the other hand, polymeric clay stabilizers like polyacrylamide (PAM) modifications or cationic organic polymers (COP) have an excellent resistance to water washout, but its anti-swelling were limited.[10,12]

To solve the above problem, more attention has been paid for the complex system of polymer and small molecules compounding.[14–16] In previous work,[17–19] we found that the acrylamide (AM) copolymer, poly (acrylamide-*co*-2-acrylamido-2-methyl propane sulfuric acid-*co*-diallyl dimethyl ammonium chloride-co-*N*-allyl heptanoic acid amide),[19] poly (acrylamide-*co*−2-acrylamido-2-methyl propane sulfuric acid-*co*-diallyl dimethyl ammonium chloride-*co*-acryl polyethers),[18] and poly (acrylamide-*co*−1-allyl-1-methylimidazolium chloride-*co*-acryl polyethers),[17] could achieve good results (the *d*-spacing could be decreased to 15.7 Å form 18.8 Å) for clay stabilizer by combining with small molecules such as KCl and NaCl. We also found that polymer molecular chain could be stretched by the negatively charged carboxyl group and the rigid benzene ring,[20] that a network structure could be formed by intermolecular association of hydrophobic groups on the polymer chain,[21] and that the network structure might contribute to reduce external water entering clay minerals and to prevent migration of clay particles.[22] In addition, it was reported that ionic liquid (trihexyl tetradecylphosphonium tetrafluoroborate) was inserted into montmorillonite (MMT),[23] as a catalyst, and could be used under high temperature (up to 150°C), which might signify that ionic liquid may be a promising small molecule for combing with polymer because of its capability to embed clay

layers.[23,24] And Sandra L. detailed the evaluation of two ionic liquids as KCl substitutes.[3,25] Nevertheless, polymer combining with ionic liquid, hasn't been reported as clay stabilizers in oil field chemicals so far.

Herein, we prepared two copolymers, using AM, acrylic acid (AA) and a functional monomer containing a hydrophobic group (*N*-allyl-2-phenoxyacetamide, APO, or *N,N*-diallyl-2-phenoxyacetamide, DAPO) as raw materials. Furthermore, the prepared copolymers combined with various imidazolium ionic liquids to achieve a complex system for clay stabilizer, and the complex solution performance, such as microstructure, rheological model and anti-swelling, were investigated.

EXPERIMENTAL

Materials

The chemicals, allyl amine and diallylamine were purchased from Nanjing Forward Chemical Reagent Factory (Nanjing, China). phenol, chloroacetic acid, AM, acrylate (AA), alkylphenol ethoxylates (OP-10), sodium sulfite ($NaHSO_3$), ammonium persulfate [$(NH_4)_2S_2O_8$], *N*-methylimidazole, bromoethane, 1-(chloromethyl)benzene, 1-bromododecane and sodium fluoroborate ($NaBF_4$) were purchased from Chengdu Kelong Chemical Reagent Factory (Sichuan, China). 2-Phenoxyacetic acid,[26] 1-ethyl-3-methylimidazolium tetrafluoroborate ([EMIM][BF_4]),[27,28] 1-dodecyl-3-methylimidazolium tetrafluoroborate ([DMIM][BF_4]),[28,29] 1-benzyl-3-methylimidazolium tetrafluoroborate ([BMIM][BF_4])[28,30] were synthesized according to literatures. HY-201S, an existing poly (acrylamide-*co*-diallyl dimethyl ammonium chloride) clay stabilizer, was purchased from Binzhou Huiyuan Petroleum Technology (Shandong, China). Other chemicals and sodium montmorillonite (Na-MMT) (Xinjiang Xiazijie Bentonite, Xinjiang, China) were commercially available and used directly without further purification.

Synthesis of APO and DAPO

7.6 g (50 mmol) of 2-phenoxyacetic acid (**1a**) was completely dissolved with 30 mL of tetrahydrofuran in a 50 mL round bottom flask, and then 6.9 mL (60 mmol) of thionyl chloride was added. The mixture was intensely stirred at 55°C for 5 h. After cooling to room temperature, the solvent and excessive thionyl chloride were removed by distillation under reduced pressure and then 2-phenoxyacetyl chloride (**2a**) was obtained. All of **2a** was dissolved in 50 mL round bottom flask with 15 mL of methylene chloride. In an ice bath, 5.4 mL (55 mmol) of allylamine or 9.2 mL (55 mmol) of diallylamine that was diluted with 10 mL of dichloromethane and 10 mL (55 mmol) triethylamine, was slowly dropped into the round bottom flask. The mixture was intensely stirred in an ice bath for 5 h to give the crude product. After successively washing by deionized water, dilute hydrochloric acid, and saturated salt solution, drying by anhydrous sodium sulfate and evaporation under vacuum, a light yellow liquid APO (83% yield) and light yellow solid DAPO (78% yield) were obtained. The synthesis routes of APO and DAPO were shown in Scheme 1.

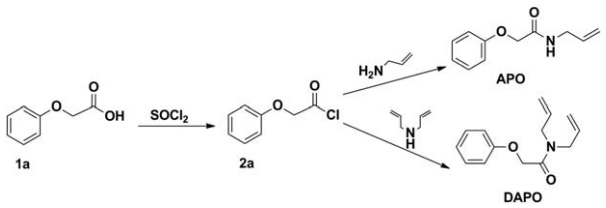

Scheme 1. The synthesis of APO and DAPO.

APO. ^{1}H NMR (400 MHz; $CDCl_3$, δ): 4.0 (dd, $J_1 = 11.4$ Hz, J_2 = 5.7 Hz, 2H, C***H***$_2$—N), 4.5 (s, 2H, OC—C***H***$_2$—O), 5.2 (t, J_1 = 27.2 Hz, J_2 = 16.9 Hz, 2H, CH_2—HC=C***H***$_2$), 5.8–5.9 (*m*, 1H, H_2C=C***H***—CH_2), 6.7 (s, 1H, N—***H***), 6.9 (*d*, $J = 8.1$ Hz, 2H, Ar-2′-***H***), 7.1 (dd, J_1 = 14.7 Hz, J_2 = 7.4 Hz, 1H, Ar-4′-***H***), 7.3 (dd, J_1 = 15.8 Hz, J_2 = 7.9 Hz, 2H, Ar-3′-***H***)ppm; ^{13}C NMR (100 MHz; $CDCl_3$, δ): 41.3, 67.3, 114.7, 116.7, 122.2, 129.8, 133.7, 157.2, 168.1 ppm.

DAPO. ^{1}H NMR (400 MHz; $CDCl_3$, δ): 4.0 (*m*, 4H, OC—C***H***$_2$—N), 4.7 (s, 2H, OC—C***H***$_2$—O), 5.1–5.3 (*m*, 4H, HC=C***H***$_2$), 5.7–5.8 (*m*, 2H, C***H***=CH_2), 6.9 (*d*, $J = 8.4$ Hz, 2H, Ar-2′-***H***), 7.0 (*d*, $J = 7.2$ Hz, 1H, Ar-4′-***H***), 7.3 (dd, J_1 = 15.1 Hz, J_2 = 7.5 Hz, 2H, Ar-3′-***H***)ppm; ^{13}C NMR (100 MHz; $CDCl_3$, δ): 47.9, 48.8, 67.3, 114.7, 117.4, 121.6, 129.5, 132.7, 158.0, 167.8 ppm.

Preparation of the AM/AA/DAPO or AM/AA/APO Copolymer

Monomers in appropriate feed composition, OP-10 (0.3 wt %, used as emulsifier), ethylene diamine tetraacetic acid (0.5 wt %, used as molecular weight modifier) and a certain amount of deionized water were taken into a three necked flask assembled with a nitrogen inlet and a magnetic stir bar. NaOH solution was added into the solution to adjust the pH. And then the reactor was kept in a water bath for 10 min at certain temperature under nitrogen atmosphere. After that, $NaHSO_3$-$(NH_4)_2S_2O_8$ initiator (indicated loading, and 1/1 mol ratio) was added and rapidly dispersed. The reactor was sealed and kept under indicated conditions for 8 h to get the crude copolymer gels. The copolymer gels were precipitated with acetone or water–ethanol and then dried in vacuum for 6–10 h to obtain the corresponding copolymers, poly (acrylamide-*co*-acrylic acid-*co*-*N*-allyl-2-phenoxyacetamide) AM/AA/APO and poly (acrylamide-*co*-acrylic acid-*co*-*N, N*-diallyl-2-phenoxyacetamide) AM/AA/DAPO. The synthesis routes of AM/AA/APO and AM/AA/DAPO were shown in Scheme 2.

Preparation of Polymer-Ionic Liquid complex

A certain amount of copolymer was dissolved in deionized water under stirring at 50°C until clear homogeneous solution was obtained. And then different amounts of IL were added in the copolymer solution and kept stirring for 4 h at 50°C until a viscous solution of polymer–ionic liquid complex was obtained.[30]

NMR Characterization

The ^{1}H NMR and ^{13}C NMR spectra of the samples were recorded by a 400 MHz Bruker AV III NMR spectrometer (Bruker BioSpin, Switzerland). Two monomers were dissolved in $CDCl_3$ and two copolymers were dissolved in D_2O.

Intrinsic Viscosity Measurement

The intrinsic viscosities [η] of the copolymers were measured with Ubbelohde viscometer at 30 ± 0.1°C.[13,20,31] The copolymers were dissolved and diluted to five different concentrations

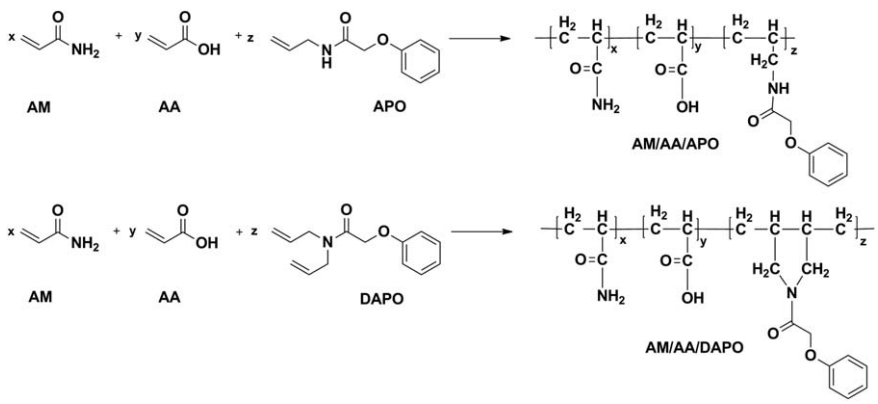

Scheme 2. The synthesis of AM/AA/APO and AM/AA/DAPO.

($C = 0.0010$, 0.00067, 0.00050, 0.00033, 0.00025 g/L) with 1 mol/L NaCl solution. The flux times of the copolymer solutions had to be accurate to ±0.2 s. The intrinsic viscosity was calculated by plotting η_{sp}/C versus C and then taking the intercept at $C = 0$ of the best fitted straight lines.

Scanning Electron Microscope

The microscopic structures of copolymer solutions of AM/AA/APO, AM/AA/DAPO, AM/AA/APO-EMIN, and AM/AA/DAPO-EMIN were investigated by scanning electron microscope (SEM). Samples (copolymer concentration = 2000 mg/L) were prepared by placing several drops of polymer solution on a special glass. Later, the solutions were frozen rapidly using liquid nitrogen. And then, the frozen samples were imaged by a Quanta450 environmental scanning electron microscope (FEI, USA).[13,22,31]

Rheological Characterization

The 2000 mg/L copolymer solutions, HY-201S or copolymer–ionic liquid complex solutions were tested by HAAKE Rheo Stress 6000 rheometer (Thermo Fisher Scientific, Waltham/Massachusetts) to get their thixotropic behaviors, their shear stress characteristics and their viscoelastic characteristics.[21]

Measurement of the Anti-Swelling Rate

The anti-swelling rates[32–34] were measured as the method provided by Natural Gas Industry Standard of the People's Republic of China SY/T 5971-94 (The evaluation method of clay stabilizer for injection fluid). According to the Natural Gas Industry Standard, 0.5 g Na-MMT was soaked in certain solution (10 mL) for 2 h. And then the solid phase and the liquid phase were separated by the supercentrifuge at 1500 RPM. At last, we measured the volume increase of the bentonite and calculated anti-swelling rate. The anti-swelling rate was determined from eq. (1).

$$\mathrm{AR} = \frac{V_W - V_P}{V_W - V_O} \quad (1)$$

In eq. (1), the V_W and V_P are the volume of swollen bentonite in distilled water and in polymer solutions. The V_o stands for the volume of dry bentonite.

X-ray Diffractometry (XRD)

According to previous reports, it was known that Na-MMT was easier to hydrate in water than other clay minerals.[4,5,11,35,36] Therefore, we took the Na-MMT as material to evaluate the ability of the copolymer to inhibit the hydration. Each solution sample (3 mL) was mixed with Na-MMT (2 g). After 1 h the changes of the interlayer spacing of the Na-MMT were determined by X-ray diffractometry (PANalytical, The Netherlands). The scattering angle (2θ) ranged from 2° to 8°.[13,22,37]

RESULTS AND DISCUSSION

The Optimizations of the Copolymerization Conditions

Initiator Content. The initiator content was discussed as shown in Figure 1(a). With the content of initiator from 0.2% to 0.4%, the apparent viscosities of the copolymers solution were increased, but with further increasing the content, the apparent viscosities were decreased. The maximum apparent viscosity could be afforded when the content of initiator was 0.4 wt % of the total monomer weight.

pH. The result from Figure 1(b) demonstrated that the best pH value for the copolymerization was 7. The pH values from 5 to 7 caused the apparent viscosities increasing. The pH values increased from 7 to 8, which caused the apparent viscosity little decrease, and the apparent viscosities decreased obviously when the pH further increased to 9.

Temperature. The temperature effect on the copolymerization was studied and summarized in Figure 1(c). It was found that the best reaction temperature was 35°C in the copolymerization. When the reaction temperature increased to 35 from 30°C, higher apparent viscosity was afforded. And increasing the reaction temperature up to 50°C, the apparent viscosity of AM/AA/DAPO and AM/AA/APO only achieved 112.7 mPa s and 51.1 mPa s, respectively.

The Total Concentration of Monomers. The effect of total concentration of monomers on copolymerization also was studied [Figure 1(d)]. It was found that the best concentration of monomers was 20 wt % in the copolymerization. Low apparent viscosity was obtained as the concentration of monomers decreased to 10 from 20 wt %. Besides, the results could not be improved when changing the concentration to 25 from 20 wt %.

The Ratio of AM to AA. The effect of different ratios of AM to AA was investigated in the copolymerization and summarized in Figure 1(e). It was found that a satisfying ratio of AM to AA was 7 : 3. Neither increasing (to 9 : 1) nor decreasing (to 5 : 5) the ratio of AM to AA could improve the apparent viscosity.

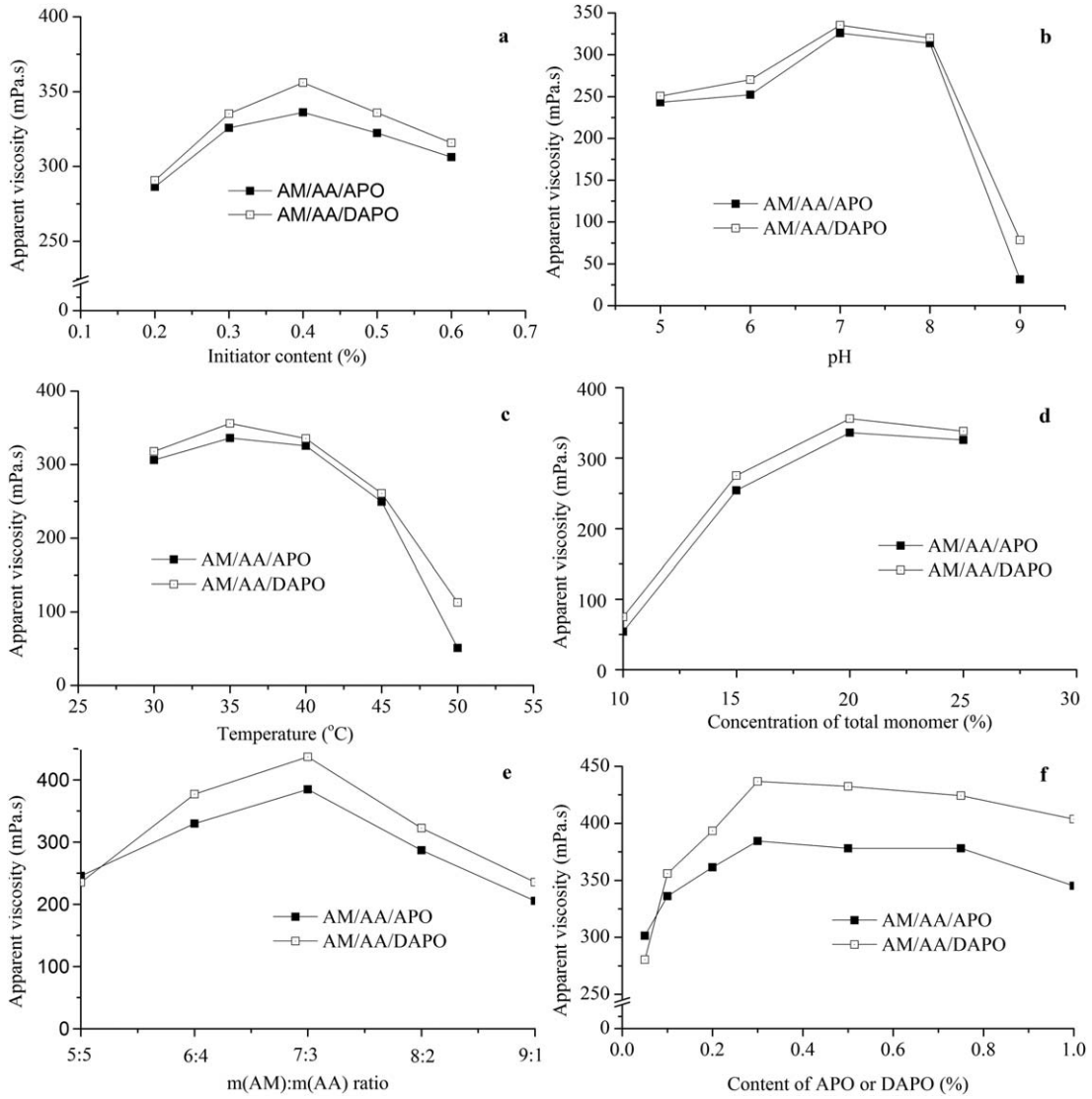

Figure 1. Effects of synthesis conditions on copolymerization.

The Content of APO or DAPO. Functional monomers could drastically improve the property of copolymers [Figure 1(f)]. The content of functional monomers form 0.05% to 0.3% could afford higher apparent viscosities. And as the content increased further, the apparent viscosity could not be improved. Therefore, the ideal loading of APO or DAPO was 0.3 wt %.

A satisfying copolymerization conditions was established, the initiator concentration was 0.4 wt %, the solution pH value was 7, the reaction temperature was 35°C, the concentration of total monomers was 20 wt %, the ratio of AM and AA on weight was 7 : 3, and the monomers APO and DAPO concentrations were 0.3 wt %, respectively. The copolymers prepared under the satisfying copolymerization condition were used for characterization and properties in this paper.

The Structural Characterization of AM/AA/APO and AM/AA/DAPO

IR. The IR spectra of APO, DAPO, AM/AA/APO, and AM/AA/DAPO are shown in Figure 2. In the spectrums of APO and DAPO, the strong characteristic peaks, 1593, 1531, 1491, 1444, 752, and 690 cm^{-1}, were assigned to the absorption of mono-

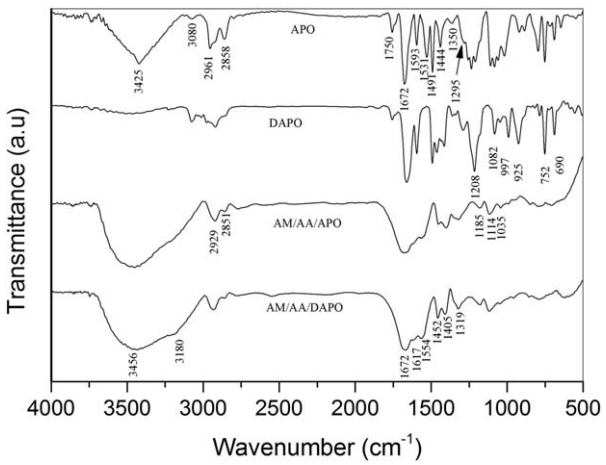

Figure 2. IR spectra of APO, DAPO, AM/AA/APO, and AM/AA/DPAO.

substituted benzene. The absorption peaks appearing at 2961 and 2858 cm^{-1} were due to the stretching vibration of C—H, in the —CH_2— group. The stretching vibration of CH_2=CH— could be observed at 1750, 997, and 925 cm^{-1}. The strong characteristic peaks (1672 cm^{-1}) were assigned to the stretching vibration of C=O. The spectrums of APO differed from DAPO at 3425 cm^{-1}, which was attributed to the absorption peak of N—H. As expected, the IR spectra confirmed the structure of APO and DAPO.

In the IR spectra of AM/AA/APO and AM/AA/DAPO, the characteristic peaks, 3456, 1617, 1554, and 1405 cm^{-1}, were due to the absorption of —COOH and —COONa. The characteristic peaks, 3180 and 1672 cm^{-1}, were due to the absorption of —$CONH_2$. The characteristic peaks, 2929 and 2851 cm^{-1}, were due to the absorption of —CH_2—. Thus, we concluded that the copolymers contained the structures of AM and AA, and that could not confirm whether the copolymers contained the structure of there DAPO or APO, which might result from the too little content of APO or DAPO. Therefore, other characterization techniques, such as NMR, should be employed.

^{1}H NMR and ^{13}C NMR. The ^{1}H NMR spectrum of AM/AA/APO was shown in Figure 3(a). In the proton spectrum, the chemical shift value at 1.6 ppm was assigned to the aliphatic —CH_2— group of main polymer chain. The proton of the aliphatic —CH— of main polymer chain appeared at 2.2 ppm. The proton of the aliphatic —CH_2— of [—CH_2—NH—CO—] appeared at 3.6 ppm. And the characteristic peak due to —CH_2— of [—CO—CH_2—O—Ph] was observed at 4.6 ppm. The chemical shift value at 6.9 ppm was due to the *ortho*-position —CH— protons of benzene ring. The chemical shift value at 7.4 ppm was assigned to the *para*-position —CH— proton of benzene ring. Signal at 7.7 ppm was due to the *meta*-position —CH— protons of benzene ring.

The ^{13}C NMR spectrum of AM/AA/APO copolymer was presented in Figure 3(b). The chemical shift value at about 35.0–36.0 ppm was assigned to the C of —CH_2— in the main chain. The C of the aliphatic —CH— of [—CH—$CONH_2$] appeared at 42.0 ppm. The C of the aliphatic —CH— of [—CH—COONa] appeared at 45.1 ppm. And the C of due to —CH_2— of [—CH_2—NH] was observed at 54.6 ppm. Signal at 69.9 ppm was due to —CH_2— of [O—CH_2—CO]. The chemical shift value at 114.1 ppm was due to the C of —CH— in the *ortho*-position of the substituent. The C of the —CH— in the *meta*-position of the substituent appeared at 126.5 ppm. The C of the —CH— in the substituent position of benzene ring appeared at 133.9 ppm. The C of [—CO—N] exhibited a signal at 179.7 ppm. The C of [—CO—ONa] exhibited a signal at 183.0 ppm.

The ^{1}H NMR spectrum of AM/AA/DAPO copolymer was shown in Figure 3(c). In the proton spectrum, the chemical shift value at 1.6 ppm was assigned to the aliphatic —CH_2— group of main polymer chain. The proton of the aliphatic —CH— of main polymer chain appeared at 2.2 ppm. The proton of the aliphatic —CH_2— of [—CH_2—N(CO)—CH_2—] appeared at 3.6 ppm. And the characteristic peak due to —CH_2— of [—CO—CH_2—O—Ph] was observed at 4.3 ppm. The chemical shift value at 6.9 ppm was due to the *ortho*-position —CH— proton in benzene ring.

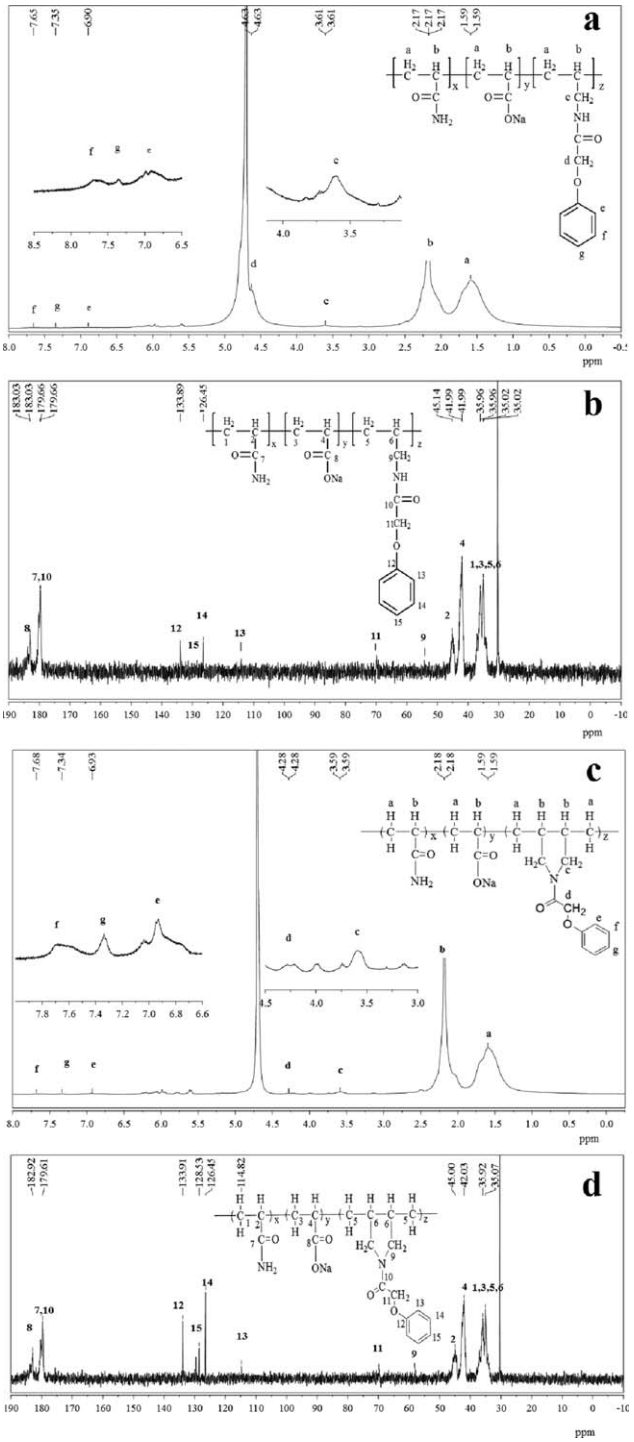

Figure 3. (a) ^{1}H NMR spectra of AM/AA/APO; (b)^{13}C NMR spectrum of AM/AA/APO; (c)^{1}H NMR spectrum of AM/AA/DAPO; (d)^{13}C NMR spectrum of AM/AA/DAPO.

The chemical shift value at 7.3 ppm was assigned to the *para*-position —CH—in benzene ring. Signal at 7.7 ppm was due to the *meta*-position —CH— proton in benzene ring.

The ^{13}C NMR spectrum of AM/AA/DAPO copolymer was presented in Figure 3(d). The chemical shift value at about 35.1–36.0 ppm was assigned to the C of —CH_2— in the main chain.

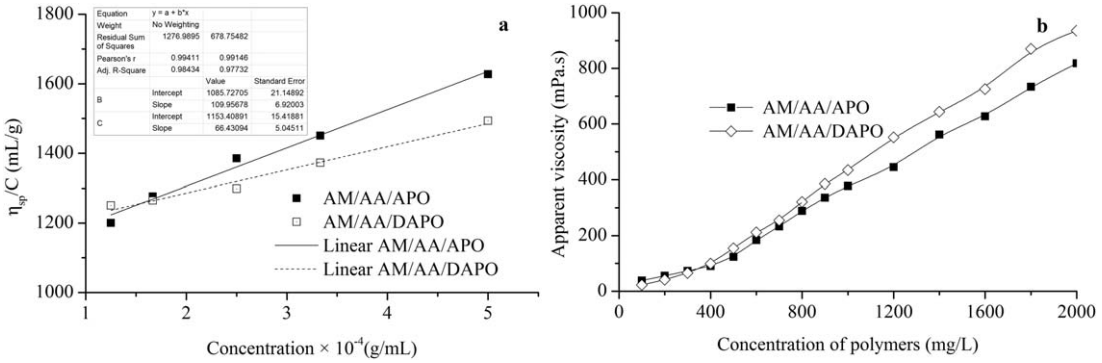

Figure 4. (a) The η_{sp}/C relationship of AM/AA/APO and AM/AA/DAPO; (a) the relationship between the apparent viscosity and concentration of AM/AA/APO or AM/AA/DAPO.

The C of the aliphatic —CH— of [—CH—$CONH_2$] appeared at 42.0 ppm. The C of the aliphatic —CH— of [—CH—COONa] appeared at 45.0 ppm. And the C of due to —CH_2— of [—CH_2—N(CO)—CH_2—] was observed at 58.5 ppm. Signal at 69.7 ppm was due to —CH_2— of [O—CH_2—CO]. The chemical shift value at 114.8 ppm was due to the C of —CH— in the *ortho*-position of the substituent. The C of the —CH— in the *meta*-position of the substituent appeared at 126.5 ppm. The C of the —CH— in the *para*-position of the substituent appeared at 128.5 ppm. The C of the —CH— in the substituent position of benzene ring appeared at 133.9 ppm. The C of [—CO—N] exhibited a signal at 179.6 ppm. The C of [—CO—ONa] exhibited a signal at 182.9 ppm.

Intrinsic Viscosity of Copolymers. The intrinsic viscosity ([η]), which reflects the expanded extent of the polymer chain, is a measurement of the hydrodynamic volume of macromolecules.[38,39] All solutions were prepared by dissolving a amount of copolymers in brine (1 mol/L), and the copolymer concentration was adjusted by adding salt solution to the flask in a constant temperature bath at 30°C.

The η_{sp}/C (concentration) relationships were plotted in Figure 4(a). It was apparent from Figure 4(a) that the intrinsic viscosity ([η]) of AM/AA/APO and AM/AA/DAPO value was 1085 and 1153 mL/g, respectively.

The Properties of AM/AA/APO and AM/AA/DAPO

Tackifying. Tackifying is one of the most important polymer performances, usually measuring by the solution apparent viscosity.[40] The apparent viscosity of AM/AA/APO solution and AM/

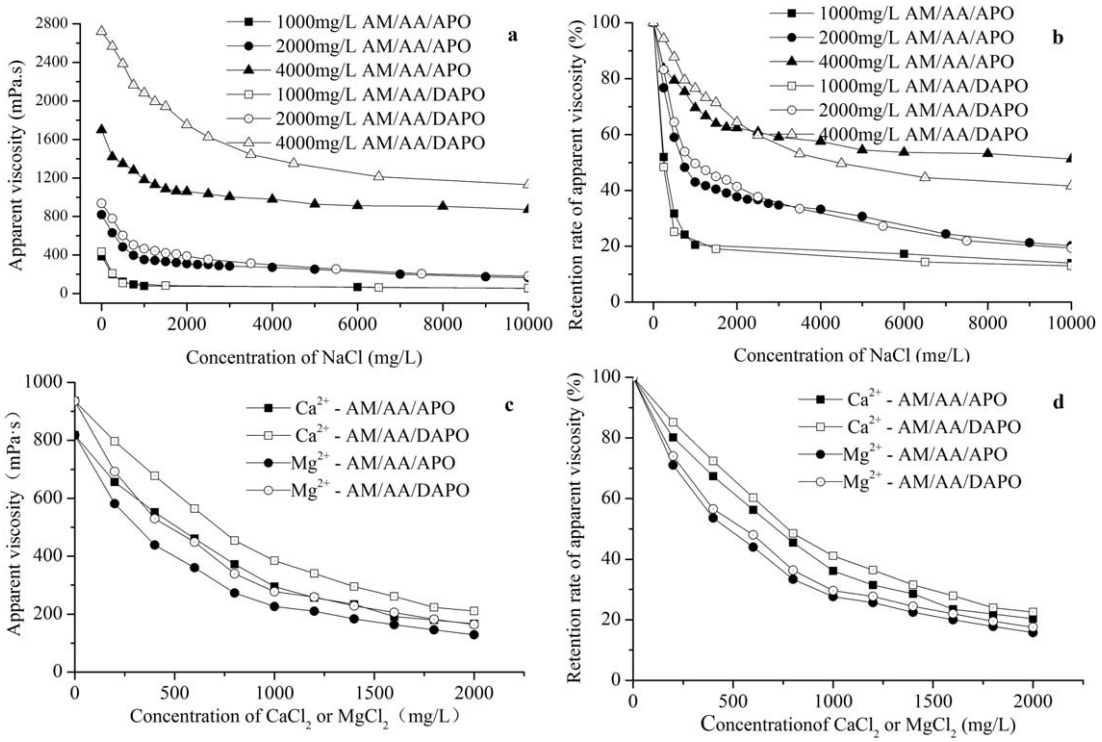

Figure 5. (a) Effect of NaCl on apparent viscosity; (b) effect of NaCl on viscosity retention rate; (c) effect of $CaCl_2$ and $MgCl_2$ on apparent viscosity; (d) effect of $CaCl_2$ or $MgCl_2$ on viscosity retention rate.

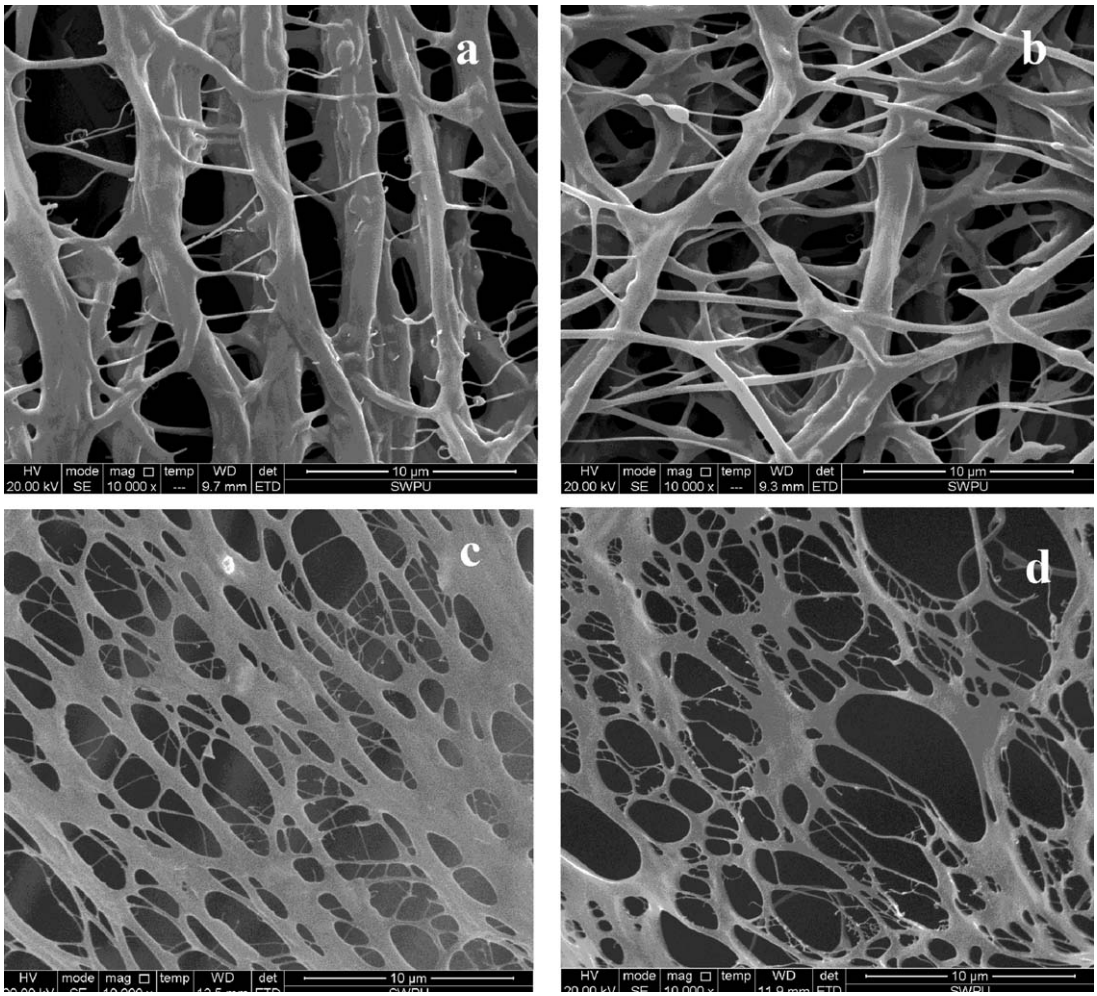

Figure 6. The SEM images of copolymers and complex: (a) AM/AA/APO solution; (b) AM/AA/DAPO solution; (c) AM/AA/APO-EMIN solution; (d) AM/AA/DAPO-EMIN solution.

AA/DAPO solution with 100–2000 mg/L copolymer was studied as shown in Figure 4(b). Seen from Figure 4(b), the apparent viscosity of AM/AA/APO solution increased slowly at 100–500 mg/L, and increased rapidly above 500 mg/L, which might result from intermolecular association. This phenomenon also appeared in AM/AA/DAPO solution below and above 400 mg/L. When the concentration of copolymer was up to 2000 mg/L, the apparent viscosity of AM/AA/DAPO solution, 935.6 mPa s, was higher than 818.4 mPa s of AM/AA/APO solution, which might cause from the network structures (shown later in SEM).

Effect of Salt. Due to various inorganic ions in the formation water, salt tolerance is also a focus of polymer properties investigatation, and sodium, calcium, and magnesium ions are usually investigated in copolymer salt tolerance.[41]

NaCl. The apparent viscosities and viscosity retention rates of copolymers solution were studied by changing NaCl content and copolymer concentrations. As Figure 5(a) showed, with the NaCl content increasing, every curve of the apparent viscosity to the NaCl content appeared an inflection region that was between the rapidly decrease and the final stabilization. And the solutions with high copolymer concentration demonstrated that the inflection region moved to the direction of high NaCl content. At same NaCl content, the solution with higher copolymer concentration retained a higher apparent viscosity, which might indicate the solution with high polymer concentration has a better salt resistance. From Figure 5(b), the viscosity retention

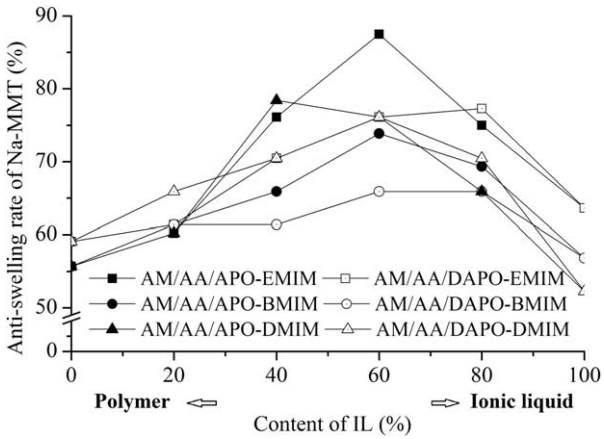

Figure 7. Effect of the preparation condition of complex.

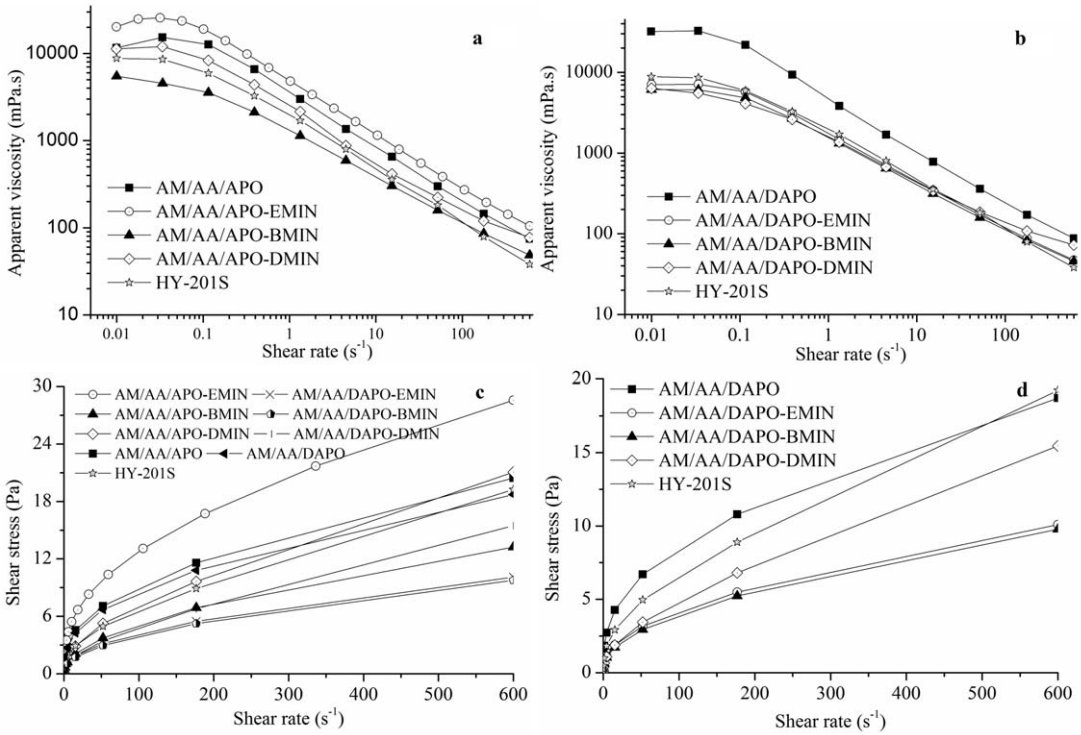

Figure 8. Effect of shearing on copolymers, HY-201S and complexes solution: (a, b) apparent viscosity and (c, d)shear stress at 25°C.

rate of the polymer solution showed similar trend with their viscosity retention vale. And the maximum apparent viscosity retention rate of copolymer solution was 51.3% (4000 mg/L AM/AA/DAPO) when the NaCl content was 10,000 mg/L. From the effect of NaCl to apparent viscosity vale and viscosity retention rate of copolymer solution, it might be seen that the intermolecular association and cross-link are helpful to improve copolymer salt tolerance.

$MgCl_2$ and $CaCl_2$. The effect of $CaCl_2$ or $MgCl_2$ on the apparent viscosity and viscosity retention rate of solution with 2000 mg/L copolymer were also investigated. The copolymer solutions, shown in Figure 5(c), demonstrated that the apparent viscosity decreased with the increasing $CaCl_2$ or $MgCl_2$ content from 0 to 1000 mg/L, and that the decrease was tapering off when the $CaCl_2$ or $MgCl_2$ content was over 1000 mg/L. Compared AM/AA/APO solution, AM/AA/DAPO solution with 1200 mg/L salt content afforded a better salt resistance, which might result from the network structure of AM/AA/DAPO solution [shown latter in Figure 6(b)]. The apparent viscosity and viscosity retention rate [Figure 5(d)] of AM/AA/DAPO solution with 1200 mg/L salt were 211.1 mPa s ($CaCl_2$), 164.0mPa s ($MgCl_2$), 22.6% ($CaCl_2$), 17.5% ($MgCl_2$), respectively.

The Preparation Conditions of Complexes

Various working fluids in petroleum exploitation may cause clay minerals swelling, which would block rock pores, so the anti-swelling property is one focus of choosing an appropriate preparation condition of complex. The anti-swelling rates of copolymers, ionic liquids, and their complexes were tested at 5000 mg/L. As shown in Figure 7, the anti-swelling rates of complexes solution were higher than that with copolymer-only or ionic liquid-only. Compared other complexes solution, AM/AA/APO-EMIN (weight ratio 40% : 60%) solution demonstrated the satisfying optimal anti-swelling rate 87.5%.

The Microstructures of the Complex Solution

The Microstructures of solution of AM/AA/APO, AM/AA/DAPO, AM/AA/APO-EMIN, and AM/AA/DAPO-EMIN at 2000 mg/L copolymer concentration were examined by SEM. Figure 6(a) demonstrated that the structure of AM/AA/APO in solution was clear linear relation between its molecules except for a small association. The structure of AM/AA/DAPO was network in Figure 6(b). The structures of two complexes in solution were thin network (Figure 6c,d), which might help to wrap clay minerals and to reduce clay particles migration.

Table I. Consistency Coefficient and Flow Behavior Index

Solutions	n ($\times 10^{-2}$)	k ($\times 10^{-2}$ Pa s^{-n})
AM/AA/APO	48.2	144.9
AM/AA/APO-EMIN	45.3	389.0
AM/AA/APO-BMIN	54.2	18.0
AM/AA/APO-DMIN	48.9	75.4
AM/AA/DAPO	41.2	230.9
AM/AA/DAPO-EMIN	50.0	18.5
AM/AA/DAPO-BMIN	51.3	14.2
AM/AA/DAPO-DMIN	55.3	15.7
HY-201S	52.9	41.3

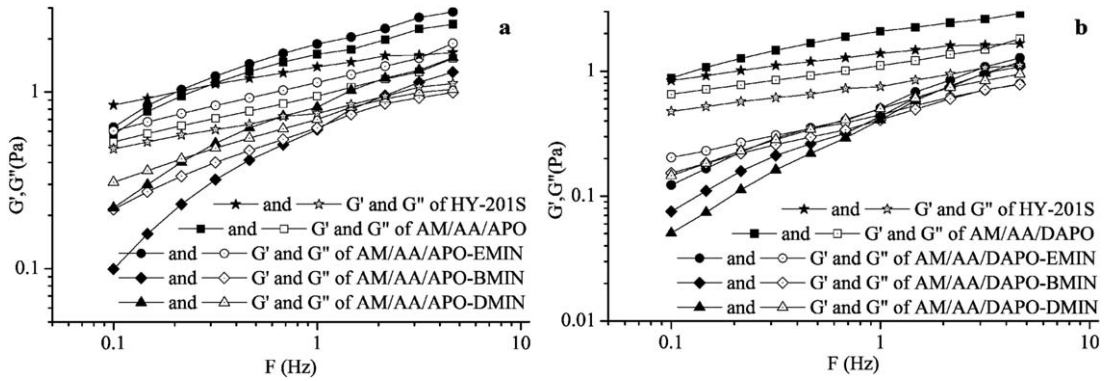

Figure 9. Effect of shearing on the storage modulus and loss modulus of copolymers, HY-201S and complexes solution.

The Properties of the Complexes

Shear Thinning. The shear thinning behavior is preferred in actual applications, because a low viscosity at high shear rates will require less pumping energy.[42] For that, the response of the copolymers, HY-201S and complexes solution at 2000 mg/L to shear from 0.01 to 600 s^{-1} were measured by an RS 6000 rheometer at 25°C. As was observed in Figure 8(a,b), with shear rate increasing, all of the solutions demonstrated a shear thinning behavior. The apparent viscosities of the complexes solution, except for AM/AA/APO-EMIN, were lower than that of their copolymer solution. When the shear rate was up to 600 s^{-1}, the viscosity retention rate of AM/AA/APO-EMIN retained 7.5% (relative to 1389.4 mPa s under 7.34 s^{-1}), which was slightly higher than the viscosity retention rate of HY-201S solution (6.5%).

Rheological Model. Mathematically, the formula is known as the power law model [eq. (2)]. It demonstrates the relationship of the shear stress (τ, Pa) with shear rate (γ, s^{-1}), which also was non-Newtonian.[43]

$$\tau = k\gamma^n \quad (2)$$

where k is the consistency coefficient (Pa s^{-n}) and n is the flow behavior index.

The flow curves of 2000 mg/L solutions of the copolymers, HY-201S and the six complexes, which accounted for the relationship between τ and γ, were shown in Figure 7(c,d). After we did a linear fitting of the graph processing, n and k were found as Table I.

Viscoelastic. The viscoelasticity of two copolymers and their complexes were studied, as shown in Figure 9(a,b). Compared the copolymers, all of their complex solutions (except for AM/AA/APO-EMIM) showed two modulus decrease. The storage modulus (G') of the two copolymers, AM/AA/APO-EMIN and HY-201S solution, were greater than their loss modulus (G''), which means the four solutions were elastic fluid.

Aging Stability. Aging stability is very important to the pilot application because the dissolved oxygen, metals, and free-radical generators in the working fluid could promote the polymer degradation.[22] We investigated the aging stability of copolymers, HY-201S and complexes solution for 15 days under 65°C. As Figure 10(a) showed, the apparent viscosity of seven solutions decreased rapidly in the first two days, and then stabilized gradually. Compared with HY-201S, AM/AA/APO and AM/AA/APO's complex solutions, the apparent viscosity of AM/AA/DAPO and its complex solutions decreased very little, which may be owing to its network structure. After 15 days of aging, the viscosity retention rate of AM/AA/APO-EMIN (84.2%) was higher than HY-201S (77.8%), which mgiht indicate AM/AA/

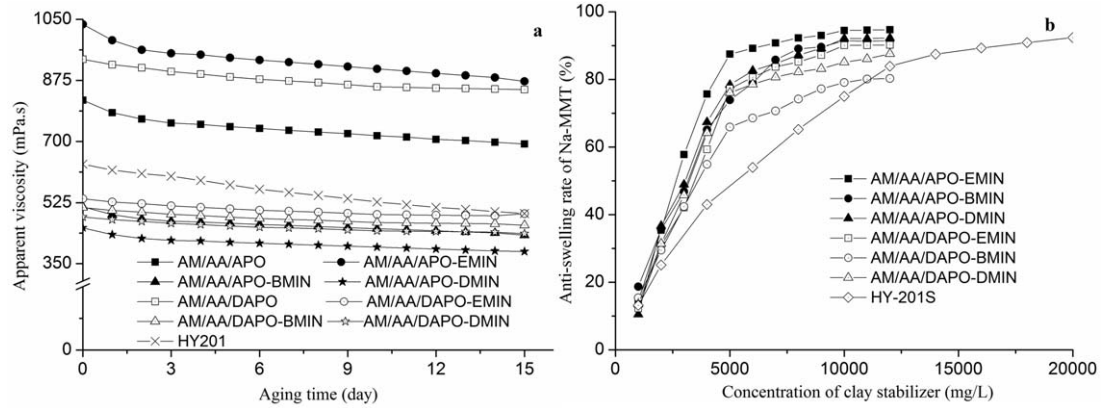

Figure 10. (a) the aging stability of complexes, HY-201S and copolymers at 65°C for 15 days; (b) effect of clay stabiliser content on anti-swelling rate.

Table II. The *d*-spacing of Na-MMT

Entry[a]	Sample[b]	*d*-spacing (Å)
1	Na-MMT[c]	12.1
2	Na-MMT-H_2O	19.1
3	Na-MMT-[EMIM][BF_4]	16.6
4	Na-MMT-[BMIM][BF_4]	17.2
5	Na-MMT-[DMIM][BF_4]	17.4
6	Na-MMT-AM/AA/APO	18.4
7	Na-MMT-AM/AA/DAPO	17.9
8	Na-MMT-40%AM/AA/APO-60%EMIN	15.7
9	Na-MMT-40%AM/AA/APO-60%BMIN	16.8
10	Na-MMT-60%AM/AA/APO-40%DMIN	16.1
11	Na-MMT-20%AM/AA/DAPO-80%EMIN	16.0
12	Na-MMT-40%AM/AA/DAPO-60%BMIN	17.0
13	Na-MMT-40%AM/AA/DAPO-60%DMIN	16.5
14	Na-MMT-HY-201S	15.9

[a] Three milliliters of solution samples was mixed with 2 g of Na-MMT and the results were tested after 3 h.
[b] The solution concentrations of copolymers, complexes or ionic liquids were 10,000 mg/L; the solution concentration of HY-201S was 14,000 mg/L.
[c] Dry Na-MMT powder.

APO-EMIN complex has a more satisfying long-term efficacy than HY-201S.

Effect of Complex Content. We investigated the effect of the complex concentration on anti-swelling rate of Na-MMT, comparing with HY-201S, to determine a reasonable content. As shown from Figure 10(b), the complex solution demonstrated that a marked increase of anti-swelling rate with concentration to 5000 mg/L from 1000 mg/L, and a slow increase with concentration above 1000 mg/L. The ideal concentration of the complex solution was about 10,000 mg/L, while that of the existing HY-201S was 14,000 mg/L, which indicated that the polymer ionic liquid complex for clay stabilizer were obvious advantages over HY-201S in content. In addition, AM/AA/APO-EMIN solution showed the best anti-swelling rate 94.5% at 10,000 mg/L.

Effect on d-Spacing of Na-MMT. We evaluated the effect of the complex solution on inhibiting the Na-MMT hydration by analyzing the change of the *d*-spacing of Na-MMT. The *d*-spacing of Na-MMT soaked by different solutions was investigated by X-ray diffraction (XRD). The results listed in Table II showed that the *d*-spacing of Na-MMT soaked by ionic liquids solution (entries 3–5), copolymer solutions (entries 6, 7), complex solutions (entries 8–13), and HY-201S (entry 14), was bigger than dry Na-MMT (entry 1) but was significantly less than that soaked by deionized water (entry 2). And AM/AA/APO-EMIN was more effective to reduce the *d*-spacing of Na-MMT (from 19.1 Å to 15.7 Å) than the existing clay stabilizer HY-201S (15.9 Å), which was consistent with the result of anti-swelling rate [Figure 9(b)]. From the above, it can be indicated that the complex cation embedding crystal layer of Na-MMT impede free water entering the crystal layer gap and reduce the expansion of *d*-spacing.

CONCLUSIONS

In this research, we got a complex system (AM/AA/APO-EMIN) for clay stabilizer, by AM/AA/APO combining [EMIM][BF_4]. And the satisfying preparation condition of complex was 60 wt % [EMIM][BF_4] and 40 wt % AM/AA/APO prepared by using AM, AA, and APO as raw materials. From SEM images, a clear network structure appeared in complex solution. AM/AA/APO-EMIN solution exhibited salt resistance (viscosity retention rate up to 51.3% at 10,000 mg/L NaCl). AM/AA/APO-EMIN solution exhibited excellent anti-swelling ability rate (up to 94.5% at 10,000 mg/L), high aging resistance (viscosity retention rate 84.2% after 15 days), and marked shear thinning behavior (viscosity retention rate 7.5% under 600 s^{-1}). In addition, the result of XRD showed that AM/AA/APO-EMIN was more effective to reduce the *d*-spacing of Na-MMT (from 19.1 Å to 15.1 Å) than the existing poly (acrylamide-*co*-diallyl dimethyl ammonium chloride) clay stabilizer HY-201S (15.9 Å). Further investigation on the applications of other ionic liquids for clay stabilizer is ongoing.

ACKNOWLEDGMENTS

The authors gratefully acknowledge the Natural Science Foundation of China (B061101) and the Sichuan science and technology plan project (2012FZ0130) for financial support.

REFERENCES

1. Zou, C.; Dong, D.; Wang, S.; Li, J.; Li, X.; Wang, Y.; Li, D.; Cheng, K. *Petrol. Explor. Dev.* **2010**, *37*, 641.
2. Shekarifard, A.; Baudin, F.; Seyed-Emami, K.; Schnyder, J.; Laggoun-Défarge, F.; Riboulleau, A.; Brunet, M.; Shahidi, A. *Geol. Mag.* **2012**, *149*, 19.
3. Seyidoglu, T.; Yilmazer, U. *J. Appl. Polym. Sci.* **2013**, *127*, 1257.
4. Zhou, Z.; Gunter, W. O.; Jonasson, R. G. paper PETSOC-95-71 presented at Annual Technical Meeting, Calgary, Alberta, 1995, June 7–9.
5. Yin, X. C.; Zhang, L. M.; Li, Z. M. *J. Appl. Polym. Sci.* **1998**, *70*, 921.
6. Boek, E. S.; Coveney, P. V.; Skipper, N. T. *J. Am. Chem. Soc.* **1995**, *117*, 12608.
7. Young, D. A.; Smith, D. E. *J. Phys. Chem. B* **2000**, *104*, 9163.
8. Callaway, R. E.; Ortiz, J.; Holcomb, D. L. paper SPE-10663-MS presented at SPE Formation Damage Control Symposium, Lafayette, Louisiana, 1982, March 24–25.
9. Baltz, T. H.; Himes, R. E.; Dalrymple, D. paper SPE-19325-MS presented at SPE Eastern Regional Meeting, Morgantown, West Virginia, 1989, October 24–27.
10. Crowe, C. W. paper PETSOC-90-07 presented at Annual Technical Meeting, Calgary, Alberta, 1990, June 10–13.
11. El-Monier, I. A.; Nasr-El-Din, H. A; Rosen, R. L.; Harper, T. L. *SPE Prod. Oper.* **2013**, *28*, 145.

12. O'Neil, B.; Maley, D. M.; Farion, G.; Giurea-Bica, G. Paper SPE-165168-MS presented at SPE European Formation Damage Conference & Exhibition, Noordwijk, The Netherlands, 2013, June 5–7.
13. Liu, X.; Jiang, W.; Gou, S.; Ye, Z.; Luo, C. *J. Appl. Polym. Sci.* **2013**, *128*, 3398.
14. Umemura, Y.; Yamagishi, A.; Schoonheydt, R.; Persoons, A. E.; De Schryver, F. *J. Am. Chem. Soc.* **2002**, *124*, 992.
15. Bon, S. A.; Chen, T. *Langmuir* **2007**, *23*, 9527.
16. Chen, H.; Chang, F. *Polymer* **2001**, *42*, 9763.
17. Liu, X.; Liu, K.; Gou, S.; Jiang, W.; Qiu, L. *Spec. Petrochem.* **2013**, *05*, 26.
18. Liu, X.; Liu, K.; Gou, S.; Ye, Z.; Liang, L.; Qiu, L. *Chem. Res. Appl.* **2013**, *10*, 1375.
19. Liu, X.; Liu, K.; Gou, S.; Ye, Z.; Liang, L.; Zhu, Z. *Chem. Res. Appl.* **2013**, *06*, 857.
20. Ye, Z.; Gou, G.; Gou, S.; Jiang, W.; Liu, T. *J. Appl. Polym. Sci.* **2013**, *128*, 2003.
21. Ye, Z.; Feng, M.; Gou, S.; Liu, M.; Huang, Z.; Liu, T. *J. Appl. Polym. Sci.* **2013**, *130*, 2901.
22. Liu, X.; Jiang, W.; Gou, S.; Ye, Z.; Feng, M.; Lai, N.; Liang, X. *Carbohydr. Polym.* **2013**, *96*, 47.
23. Byrne, C.; McNally, T. *Macromol. Rapid. Commun.* **2007**, *28*, 780.
24. Selvam, T.; Machoke, A.; Schwieger, W. *Appl. Catal. A Gen.* **2012**, *445*, 92.
25. Kim, N. H.; Malhotra, S. V.; Xanthos, M. *Micropor. Mesopor. Mat.* **2006**, *96*, 29.
26. Nagy, G.; Filip, S. V.; Surducan, E.; Surducan, V. *Synth. Commun.* **1997**, *27*, 3729.
27. Lucas, P.; EI Mehdi, N.; Ho, H. A.; Belanger, D.; Breau, L. *Synthesis* **2000**, *9*, 1253.
28. Wang, Y.; Shang, Z. C.; Fan, T. X.; Chen, X. *J. Mol. Catal. A* **2006**, *253*, 212.
29. Magill, A. M.; McGuinness, D. S.; Cavell, K. J.; Britovsek, G. J.; Gibson, V. C.; White, A. J.; Williams, D. J.; White, A. H.; Skelton, B. W. *J. Organomet. Chem.* **2001**, *617*, 546.
30. Kataria, S.; Chaurasia, S. K.; Singh, R. K.; Chandra, S. *J. Phys. Chem. B* **2013**, *117*, 897.
31. Gou, S.; Liu, M.; Ye, Z.; Zhou, L.; Jiang, W.; Cai, X.; He, Y. *J. Appl. Polym. Sci.* **2014**, *131*, 4221.
32. Wong, R. C. K. paper ISRM-9CONGRESS-1999-162 presented at 9th ISRM Congress, Paris, France, 1999, August 25–28.
33. Madsen, F. T.; Nuesch, R. Paper ISRM-7CONGRESS-1991-057 Presented at 7th ISRM Congress, Aachen, Germany, 1991, September 16–20.
34. Wever, D. A. Z.; Picchioni, F.; Broekhuis, A. A. *Eur. Polym. J.* **2013**, *49*, 3289.
35. Al-Khanbashi, A.; Abdalla, S. W. *Geotech. Geol. Eng.* **2006**, *24*, 1603.
36. Fan, Z. Z.; Li, C. *Adv. Mater. Res.* **2012**, *430*, 345.
37. Liu, X.; Shu, L; Liu, H.; Wu, X. *J. Rock Soil Mech.* **2011**, *1*, 79.
38. Alagha, L.; Wang, S.; Xu, Z.; Masliyah, J. *J. Phys. Chem. C* **2011**, *115*, 15390.
39. Wever, D. A. Z.; Picchioni, F.; Broekhuis, A. A. *Eur. Polym. J.* **2013**, *49*, 3289.
40. Seright, R. S.; Campbell, A. R.; Mozley, P. S.; Han, P. H. *SPE J.* **2010**, *15*, 341.
41. Ma, S.; Liu, M.; Chen, Z. *J. Appl. Polym. Sci.* **2004**, *93*, 2532.
42. Al-Fariss, T.; Pinder, K. L. *Can. J. Chem. Eng.* **1987**, *65*, 391.
43. Zhang, L.; Zhang, D.; Jiang, B. *Chem. Eng. Technol.* **2006**, *29*, 395.